Journal of Balkan Science and Technology

journal homepage: www.jbst.nku.edu.tr/

Investigation of the Applicability of Thermoset Polyurethane Resin in Automotive Bushing Systems

Pelin GULER[1], Egemen BAYRAMLAR[1], Kenan CINAR[1*], Ahmet KAYMAZ[2], Elçin KAHRAMAN[2], Bülent Ecevit BAYRAM[2], Sezer GELEN[2]

[1] Department of Mechanical Engineering, Corlu Engineering Faculty, Tekirdağ Namık Kemal University, 59860, Çorlu-Tekirdağ, TÜRKİYE
[2] Sio Automotive, Ergene-Tekirdağ, TÜRKİYE

Research Article	**ABSTRACT**

Rigid polyurethane materials (PUR) form an important subgroup of polymeric materials. These materials are produced by gradual polyurethane reactions of isocyanates and compounds called polyols containing hydroxyl groups. These basic reactions lead to many products with various properties of polyurethanes that can be used for different purposes. The diversity of the obtained forms of PUR is possible by changing the raw materials and their mixing ratios. In this study, it was investigated whether the polyurethane bushings we produce can be used instead of the rubber bushings that are widely used today. In order to make the mechanical properties of polyurethane bushings similar to rubber bushings, the amount of hardening resin was changed and glass ball, SLES, and carbon powder materials were added. Test results showed that carbon fiber powder improved the strength and ductility of polyurethane, enhancing bushing performance. Glass beads increased ductility but reduced tensile and compressive strength. The addition of SLES caused polyurethane to foam, preventing the achievement of desired strength values. Polyurethane's tensile strength increased with strain rate, but the elongation decreased. Under tensile loading, polyurethane was more sensitive to strain rate. In fatigue testing, stiffness decreased over time in the tensile region but remained constant in compression. Bushing production using the casting method passed durability tests, indicating that polyurethane resin could serve as an alternative to the traditional rubber in automotive applications.

1. Introduction

The bushing system in a car's suspension system plays a vital role in reducing vibrations, minimizing noise transmission, and enhancing overall ride quality. As the key components that allow relative movement between interconnected parts, bushings facilitate controlled movement while damping oscillations caused by road irregularities. By providing a flexible interface between components such as control arms, sway bars, and subframes, bushings reduce shocks and vibrations, thereby improving passenger comfort and strengthening vehicle stability. Additionally, they enhance steering precision and handling response by reducing unwanted chassis flex and maintaining optimal alignment geometry.

It is a well-established fact that rubber bushings subjected to multi-axial mechanical loads degrade over time. Consequently, it is crucial to design and manufacture rubber bushings that can withstand challenging environmental conditions. As noted by Mars and Fatemi [1,2], numerous experiments have been conducted to enhance the durability of rubber materials. Typically, the fatigue life of a component is evaluated using three methods. The first method involves determining the complete fracture limit through crack propagation. Since approximately 90% of the test duration is spent on crack formation, this phase is referred to as the

complete fracture time, marking the end of the rubber material's service life. The second method permits the formation of some cracks during testing. The third method, as employed by Ostoja-Kuczynski and Charrier, is applied in displacement- and load-controlled experiments. In this method, the ratio of the maximum force in one cycle to the maximum displacement is determined [3].

After examining the methods that determine fatigue life, it is essential to consider the influencing factors. Factors affecting fatigue life can be divided into three categories. The first is mechanical loads. Rubber parts are typically not subjected to static loads during testing. Tests conducted under static loads do not closely resemble actual conditions. Mechanical tests include tension-compression, tension-torsion, compression-compression, and compression tests. The loads can be applied with constant or variable amplitude. Some researchers have conducted tests with constant amplitude [4-6], but variable amplitude provides more accurate results [7]. Otherwise, the fatigue life of the rubber bushing part has been found to exceed the calculated fatigue life. When comparing the fatigue cracks of NR (Natural Rubber) and SBR (Styrene Butadiene Rubber), the results are similar, but SBR shows fewer surface cracks than NR. It has been observed that the steps of

* Tekirdağ Namık Kemal University, Çorlu Engineering Faculty, Department of Mechanical Engineering, Silahtarağa Mah. Universite 1 sok, No:13 59860, Çorlu-Tekirdağ, TÜRKİYE
E-mail address: kcinar@nku.edu.tr

crack formation are very similar for both types of rubber. Furthermore, tests involving temperature, rubber thickness, and complex loading have shown that crack growth increases as the temperature rises; although stress increases with thicker rubber, fatigue life improves, and crack formation decreases. However, significant differences in thicknesses yield meaningful results, and various typical tests have been discussed for complex loading conditions where fundamental parameters of rubber fatigue were extracted [8]. Secondly, chemical compositions play a role. It has been observed that the type of rubber directly affects chemical compositions. NR, due to its high strength, has been a subject of interest for many researchers [9-12]. Le Cam et al. conducted a static uniaxial test on natural rubber reinforced with carbon black and observed small crack paths forming [9]. The crystallizations positively impact fatigue life. Secondly, SBR has gained popularity among researchers. The effects of SBR on fatigue cracking, the impact of antioxidants on the growth of SBR fatigue cracks, and the initiation and progression of fatigue cracks on the surface of SBR have been studied [13-15]. CR (Chloroprene) is another subject of investigation. For this type of rubber, it was observed that as the force increases, hardness decreases. In areas where hardness decreases, strain occurs, and crystallization increases, leading to more fractures [16,17]. In addition, studies on NR/BR and NR/SBR blends have shown that NR/BR exhibits better strength and superior crack resistance [5]. In recent scientific studies and industrial applications, SBR/BR/NR blends have become common. The effects of this tri-blend on fatigue behavior have been investigated, and it was concluded that it offers superior crack growth resistance [18]. The third factor influencing fatigue life is environmental conditions. In addition to mechanical loading, environmental factors also contribute to the lifespan of rubber components. It is particularly emphasized that rubber's exposure to oxygen in the air leads to chemical damage. Moreover, temperature fluctuations impact the mechanical properties of rubber, and exceeding optimal temperature limits causes degradation. Various findings have been presented on how thermal aging [19] affects rubber's mechanical properties. In some cases, thermal aging improves mechanical properties, while in others, it worsens them. Especially, thermo-oxidative aging [20-22] has been found to increase rubber's sensitivity to temperature and increase linearly with aging time [23]. Additionally, studies on how ozone affects rubber and the effect of aluminum powder on improving ozone resistance have been addressed. It has been noted that aluminum-filled rubber increases ozone resistance compared to unfilled rubber and reduces crack formation [24].

Thermoset polyurethane material can be an alternative to the traditional rubber system used in bushing systems. The use of thermoset polyurethane in bushing systems is a strategic engineering choice to optimize performance, durability, and resistance in automotive suspensions. Its inherent flexibility enhances ride comfort by effectively dampening vibrations and shocks while reducing noise transmission. Additionally, its resistance to oils, fuels, and environmental factors ensures long-lasting usage, reduces maintenance requirements, and increases overall reliability [25]. Thermoset polyurethane materials have occasionally been used in bushing systems [25-27]. Junik et al. [25,26] examined two different polyurethane materials with hardness levels of 80 and 90 ShA in the suspension system of a

sports car. They found that both materials were extremely sensitive to notch configurations, and the 90 ShA material had a better fatigue durability limit compared to the 80 ShA material. In a study by Cerit et al. [27], thermoset polyurethane material was used in a sway bar. They concluded that adjusting the bushing could increase the sway bar's fatigue life, leading to a significant reduction in equivalent stress. It was noted that selecting a softer rubber material compared to the original bushing could provide an approximately 9% improvement. Similarly, increasing the wall thickness from 7 mm to 8.75 mm for a material with 75 Shore A hardness resulted in an 11% improvement.

In this study, thermoset-based polyurethane material that can demonstrate durability comparable to rubber bushings was developed using various reinforcements, and suitable bushing mold designs were made for the material. Tensile, compression, hardness, and fatigue tests were conducted on the materials produced within the scope of the study.

2. Material and Method

2.1. Metarials Used

In this study, EN 2100-70 polyurethane resin and hardener were used. It is a casting resin equivalent to flexible polyurethane rubber. The flexible polyurethane casting resin has high elasticity, is tear-resistant, and has a hardness of 70 Shore A. The storage conditions require that they always be kept in a closed and dry environment, with a room temperature of at least -15°C, as they are highly sensitive to moisture. Two methods were used to change the mechanical properties of the polyurethane material according to their requirements. In the first method, the amount of hardener was varied. In the second method, carbon fiber powder, SLES material, and glass microspheres were added in different proportions. The particle size of the carbon powder used ranges from 100 to 400 microns. It is used in applications where electrical resistance, high wear resistance, and buckling strength are desired. The glass beads are produced from soda-lime glass and have an average diameter of 20 microns. While being an inert product, it does not dissolve in water. Sodium Lauryl Ether Sulfate (SLES) is an anionic detergent and a surfactant. It is a highly effective foaming agent. It is a paste that can be pumped at room temperature. It forms a high-viscosity gel at concentrations ranging from 28% to 65%. KP powder pigment has been added to give different colors to the bushings.

2.2. Manufacturing of Samples

In cases where no additives were added, the polyurethane resin and hardener were mixed for 3 minutes until homogeneous at the specified ratios. In samples where additives were used, the polyurethane and reinforcement material were first mixed until a homogeneous form was achieved, after which the hardener was added and mixed for 3 minutes until a homogeneous consistency was reached. To minimize the amount of air bubbles formed during the mixture, the prepared mixture was kept in a vacuum oven before being poured into the mold cavities. The mixture ratios prepared for the samples are provided in Table 1. In the sample coding given in the table, "P" represents polyurethane, the following number represents the hardener ratio, the subsequent letter group represents the type of

Table 1. Mixing ratios

Name	Hardener resin amount	Glass Globule 20μ	Sles	Carbon Fibre Powder 100-400μ
P40	%40			
P50	%50			
P40C5	%40	%5		
P40C10	%40	%10		
P40SLESD1	%40		1 drop	
P40KE5	%40			%5
P40KE10	%40			%10

additive, and the last number represents the ratio of the amount of additive. "C" represents glass beads, "SLES" represents the SLES material, and "KE" represents powdered carbon fiber.

The samples and molds used in the study are shown in Fig. 1. For the metal molds, commonly available 1040 steel was used. Metal mold designs were created using SolidWorks
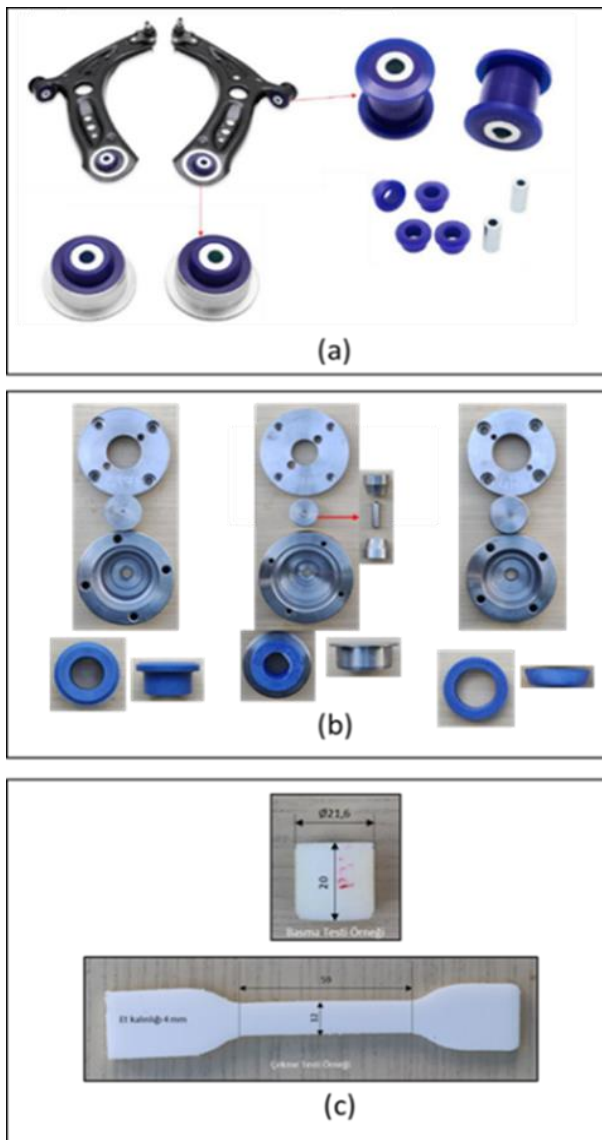
Fig. 1 (a) Bushing systems, **(b)** metal moulds and samples of bushings, **(c)** tensile and compression specimens.

Software. The molds were produced using turning processes. Silicone material was used for the tension and compression molds.

2.3. Testing Methods

In the compression test, a Zwick brand 10-ton electromechanical testing machine was used (Fig. 2(a)). Compression test samples, prepared to be 20 mm in length, were subjected to testing at a speed of 2 mm/min up to 15 mm. To prevent bulging in the samples during the test, grease was applied to both the top and bottom of the sample. Tensile tests were carried out at various speeds using a Tinius Olsen H25KS brand 500 kg capacity electromechanical device (Fig. 2(b)). Fatigue tests were conducted using an MTS brand servo-hydraulic testing machine (Fig. 2(c)). The fatigue tests were performed at 4 Hz with a load limit of ±1.8 kN, and load-displacement data were recorded. Hardness measurements were taken on the Shore A scale. For all tests, graphs were prepared based on the average of a minimum of three samples.

3. Results and Discussion

3.1. Test Speed Effect

Samples produced were subjected to tensile and compression tests at different speeds. Fig 3 presents the tensile test results for P40 and P50 polyurethane materials at speeds of 5 mm/min, 50 mm/min, and 500 mm/min. Three samples were tested from each set, but the graphs here show average curves representing the sample behaviors. For both sample sets (P40 and P50), it was observed that as the test speed increased, the strength of the samples increased, although the unit elongation at break value decreased. The lowest unit elongation at break value for both samples occurred at a speed of 50 mm/min. The effect of test speed was also evaluated for samples with added carbon fiber powder. P40KE5, P40KE10, and P40KE15 samples were tested at different speeds, and the stress-strain curves are presented in Fig 4. In these sample sets, as the test speed increased, the strengths of the samples increased. Additionally, with the addition of carbon fiber powder, the unit elongation at break value also increased as the test speed increased. Compared to plain polyurethane, carbon fiber powder exhibited a positive effect on both strength and elongation at high speeds.

The same situation was applied for compression tests, and the compression stress and strain curves for P40KE5, P40KE10 and P40KE15 samples at different speeds are presented in Fig 5. Compression tests were conducted only at speeds of 5 mm/min and 50 mm/min. As seen from the stress-strain curves, the effect of speed under compressive load is very low compared to tensile load and can be considered negligible. The increase in carbon fiber content did not visibly change the effect of speed either. From this, it can be concluded that polyurethane material is more sensitive to strain rate under tensile load. Additionally, as the speed increased under tension, the strength of the material and its rigidity in the second nonlinear region also increased.
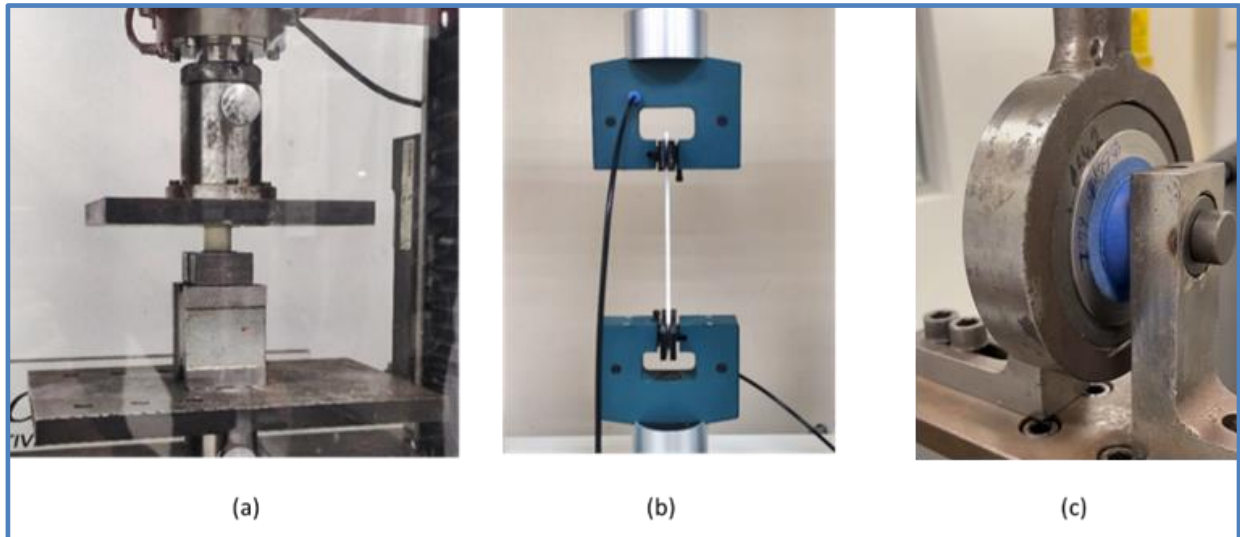
Fig. 2 Tests, **(a)** Compression test, **(b)** Tensile test, **(c)** Fatigue test.
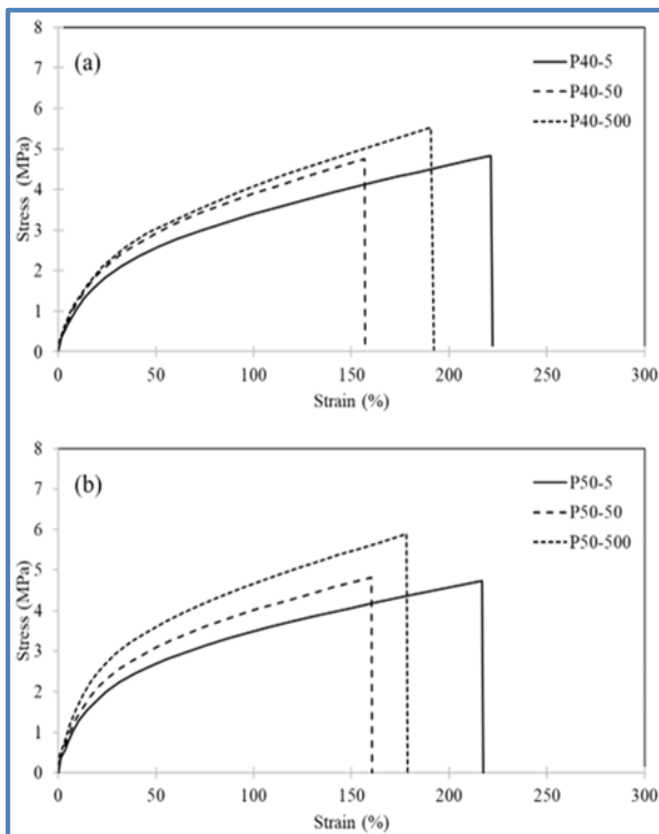

Fig. 3 Stress-strain curves of P40 and P50 samples.
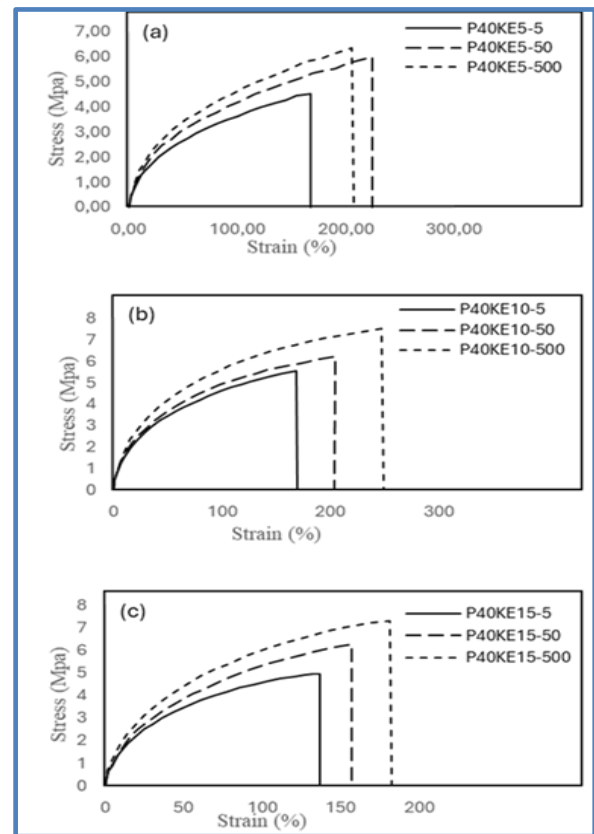

Fig. 4 Tensile tests of P40KE5, P40KE10, and P40KE15 samples at different speeds: **(a)** 5 mm/min, **(b)** 50 mm/min, and **(c)** 500 mm/min.
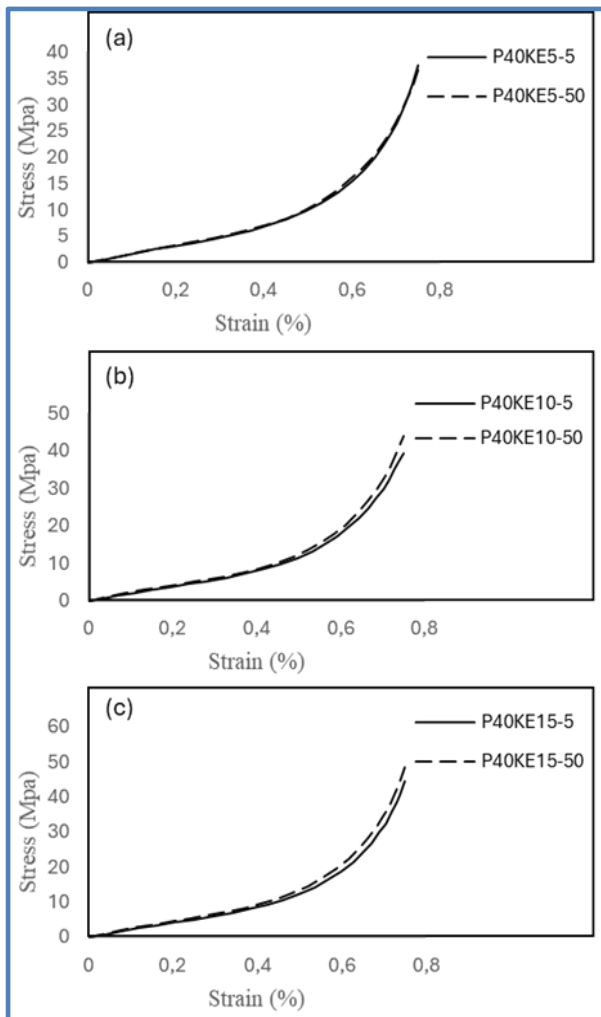
Fig. 5 Compression tests of (a) P40KE5, (b) P40KE10, and (c) P40KE15 samples at speeds of 5 mm/min and 50 mm/min.

3.2. Hardener-Resin Ratio Effect

The manufacturer's recommended weight ratio of hardener to resin is 40/100. Research in the literature indicates that changing the amount of hardener can both increase and decrease strength and deformation. In this study, samples were prepared to determine how different ratios of hardener (%35, %40, and %50) affect compressive and tensile behavior, and these samples were subjected to compression and tensile tests. Figure 6 presents the results of the compression tests for P35, P40, and P50. As shown in the figure, when the hardener amount is increased from %40 to %50, the strength value at the given strain increased by %63. Similarly, when the hardener amount was decreased to %35, the strength value decreased by %88. When the compressive load on the samples was removed, P40 and P50 returned to their original form, while P35 became deformed. The final states of the samples are shown in Fig. 6. On the other hand, there is no observable difference in the tensile behavior as shown in Fig. 7 for P40 and P50.

3.3. Effect of inclusions on mechanical properties

The effect of carbon fiber powder, glass beads, and SLES materials on the mechanical properties of polyurethane was investigated. The impact of carbon fiber powder under compressive load is shown in Fig. 8. As seen in the figure, with the increase in carbon fiber powder, the compressive strength significantly increased, and with a %15 addition, the strength value increased by %30. Additionally, when the compressive load was removed, the sample returned to its original state. The behavior under tensile load is presented in Fig. 9. Carbon fiber powder also increases tensile strength under tensile load, with a %15 addition resulting in a %32 increase in tensile strength. Furthermore, the unit elongation at break does not decrease; in fact, the unit elongation values at break increase at lower addition rates. For example, the maximum deformation was achieved with a %5 addition.
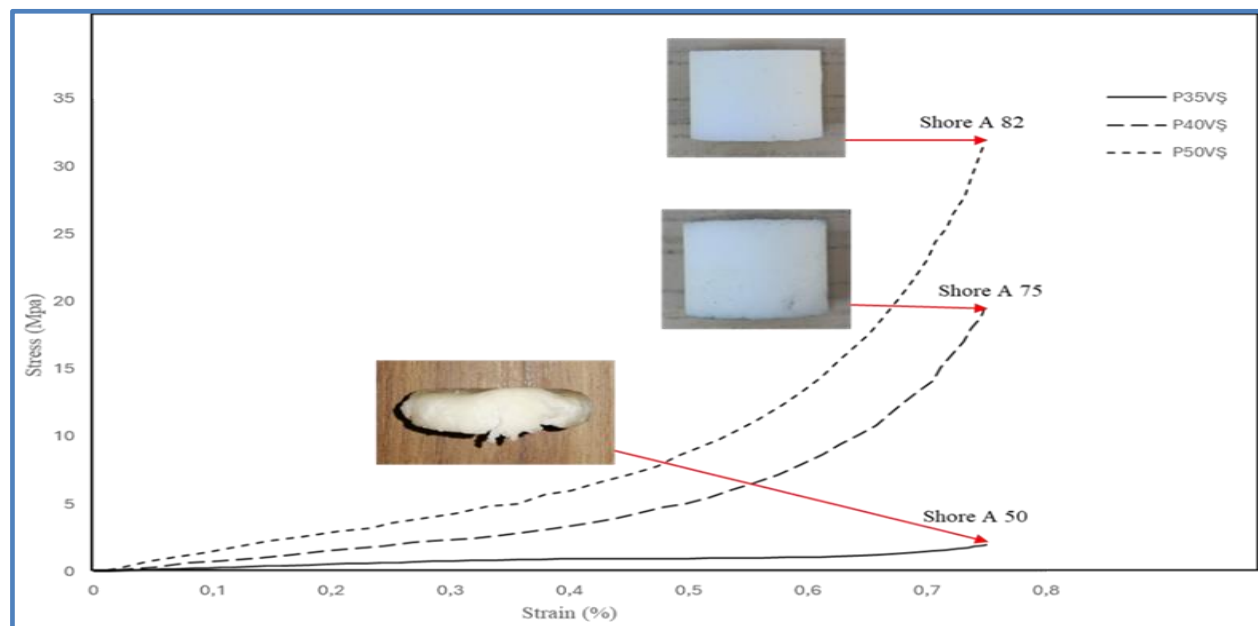
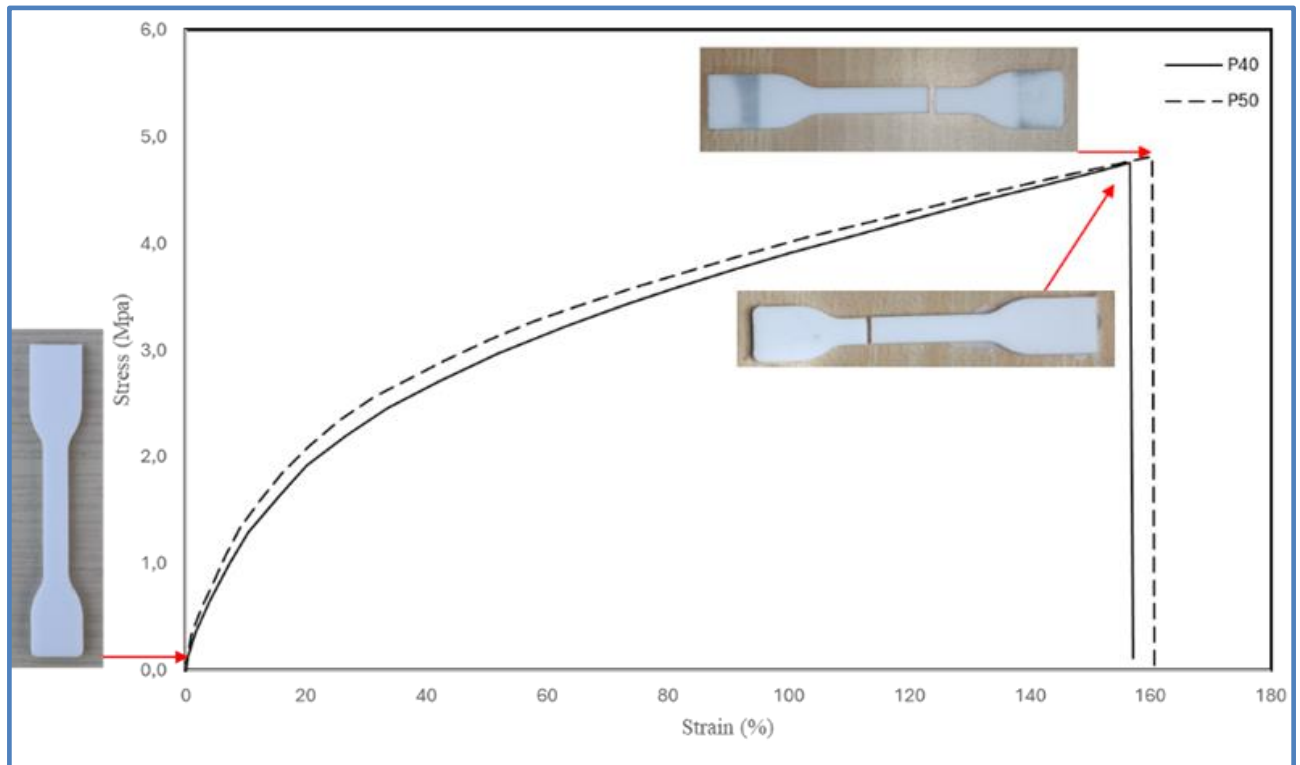

Fig. 6 Stress-strain curves for P35, P40, and P50.

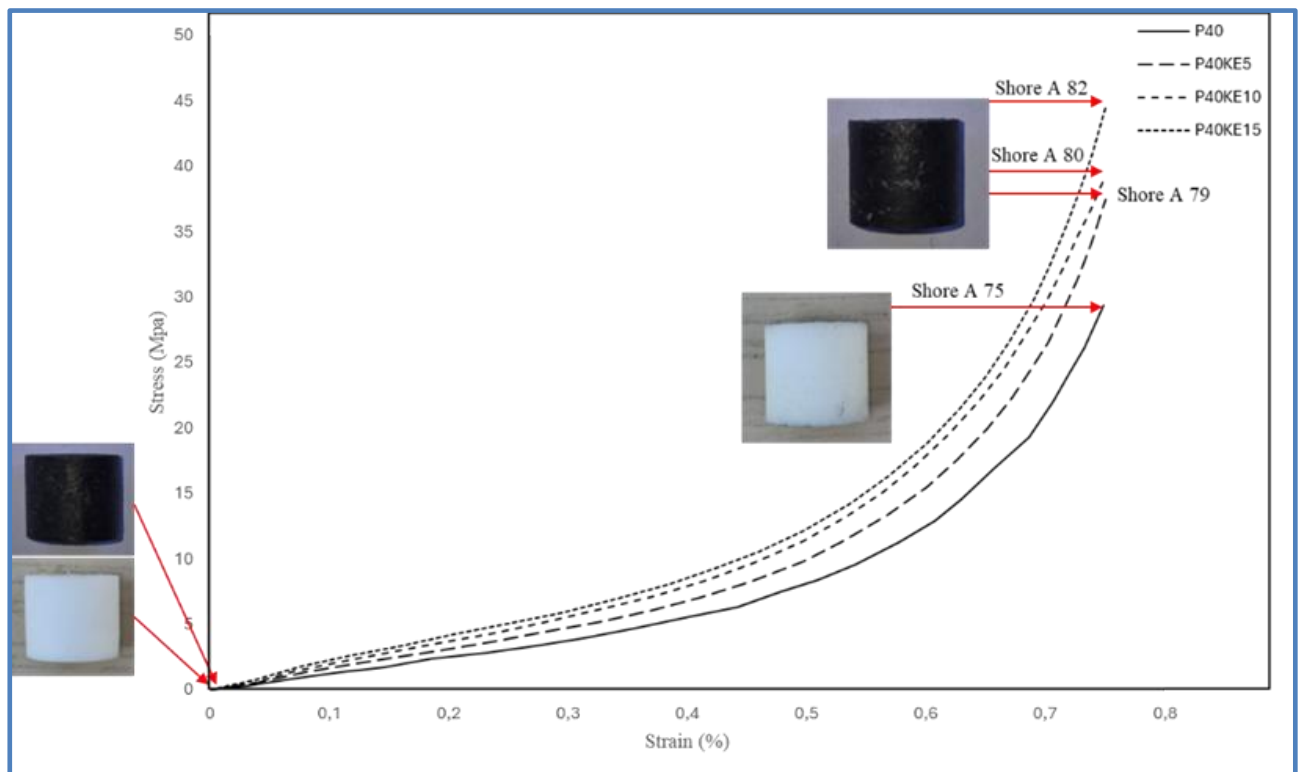**Fig. 7** Comparison of P40 and P50 samples under tensile load.

Fig. 8 Effect of carbon fiber powder on stress-strain behavior under compressive load**.**
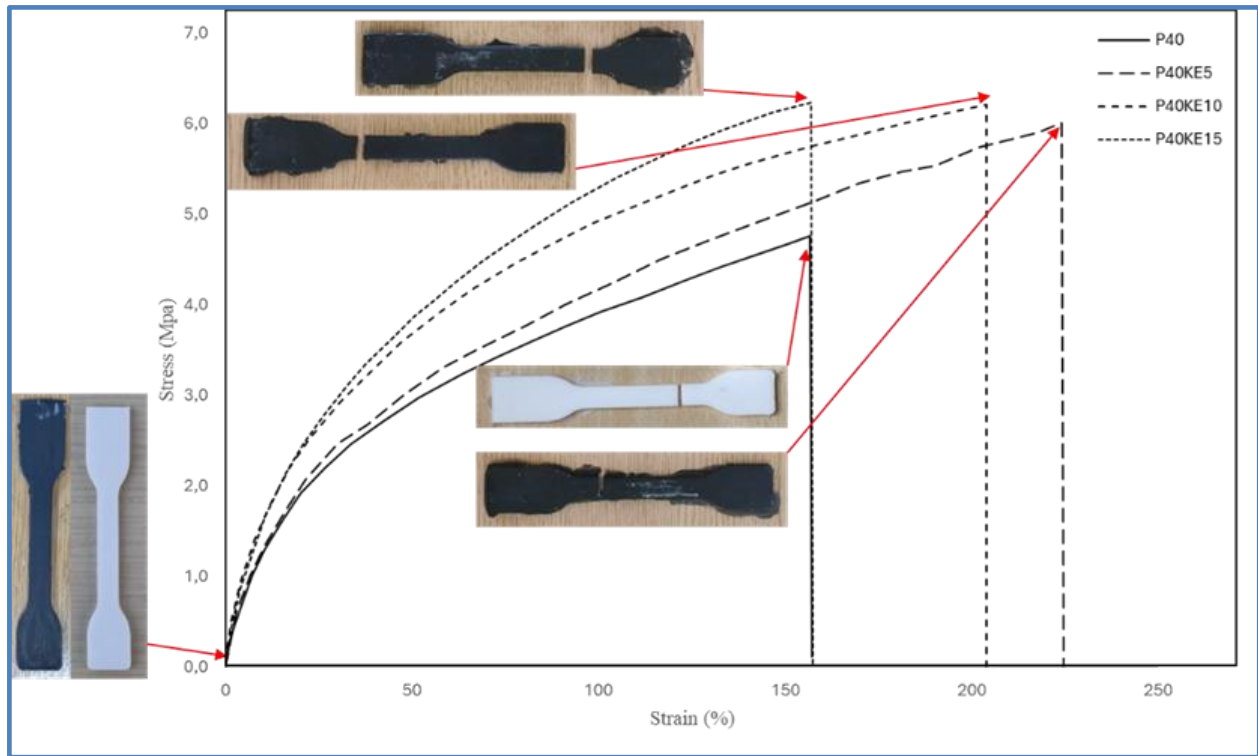
Fig.9. Effect of carbon fiber powder on stress-strain behavior under tensile load.
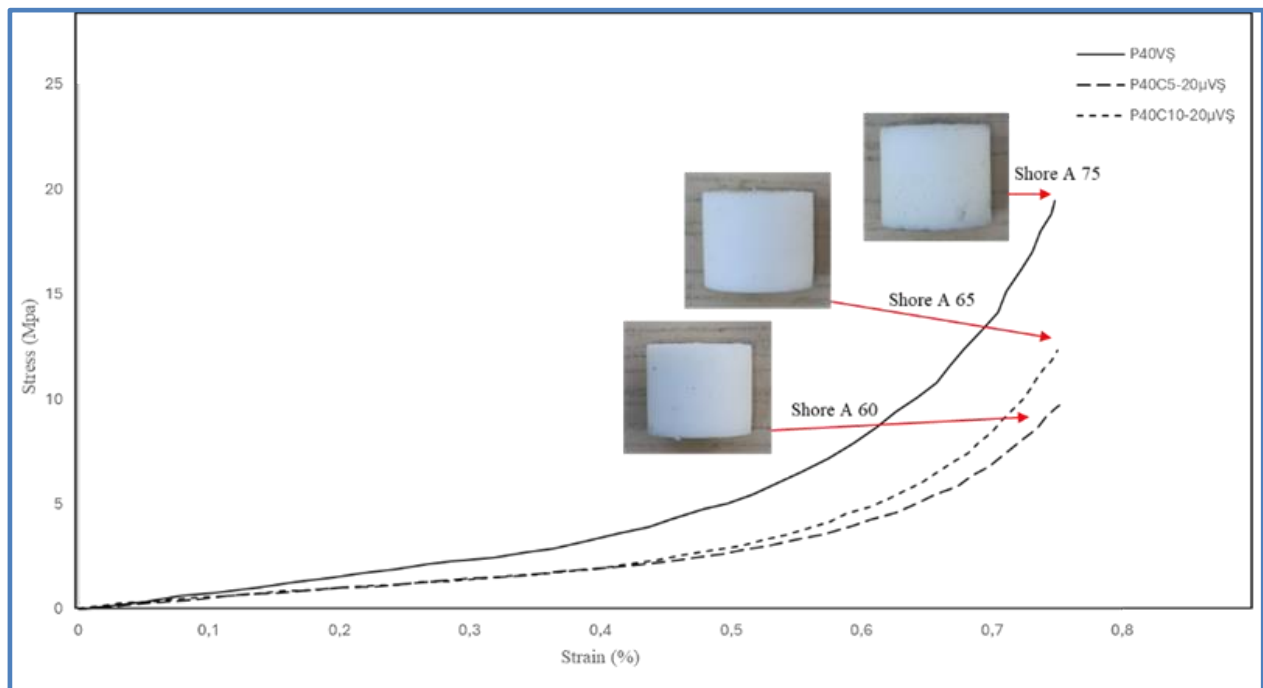

Fig.10. Effect of glass bead additive material on stress-strain behavior under compressive load.

P40 material was supplemented with 20 μm sized glass beads at %5 and %10 ratios, and their behavior under compressive load is shown in Fig. 10. As can be seen in the figure, the addition of glass beads has reduced the compressive strength. The P40C5 sample showed a strength reduction to 9 MPa, indicating a %53 decrease. The P40C10 sample decreased to 12.5 MPa, representing a %34 reduction. Similarly, the Shore A hardness values for P40C5 and P40C10 were measured as 63 Shore A and 65 Shore A, respectively. The Shore A value of the base material (P40) was measured at 70. Tensile samples with %5 glass bead additive (P40C5) were also produced, and tensile tests were conducted. Fig. 11 presents the stress-strain curve for
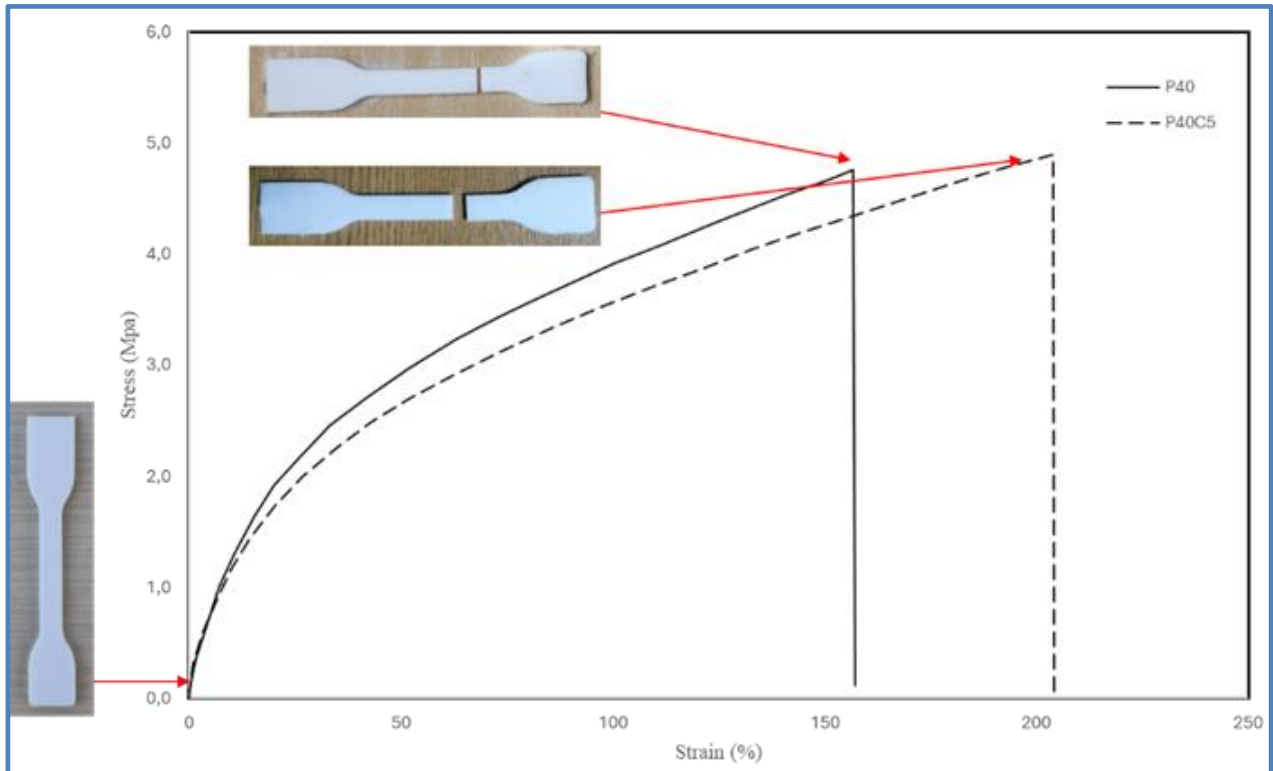
Fig. 11 Effect of glass bead additive material on stress-strain behavior under tensile load.
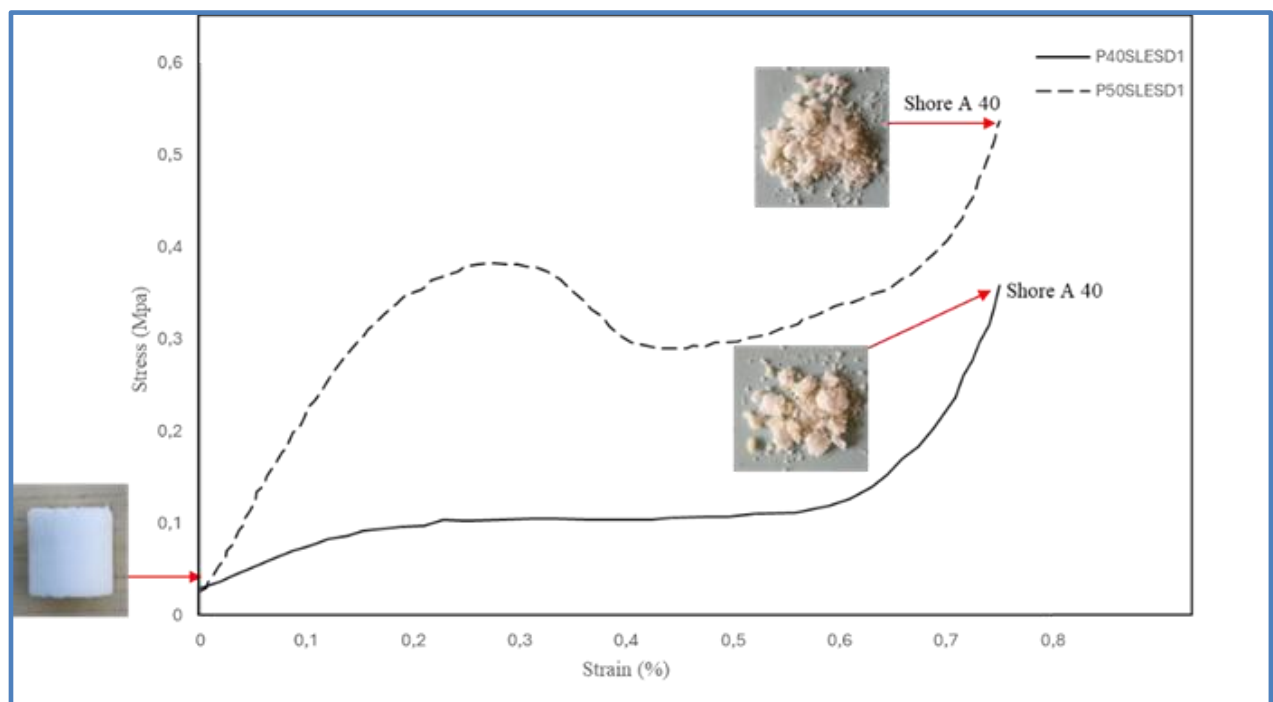

Fig. 12 Behavior of SLES-containing P40 and P50 materials under compressive load.

the P40C5 sample. A %2 increase in tensile strength was observed for the P40C5 sample. Additionally, a %32 increase in unit elongation at break was achieved. Under compressive loading, the rigid glass beads create localized stress concentrations, leading to early microcrack formation and premature failure, thereby reducing compressive strength. Additionally, weak interfacial bonding between the polymer matrix and the glass beads can hinder load transfer, further compromising structural integrity. The presence of glass beads may also introduce voids or weak points, which negatively impact the material's ability to resist compressive forces. In contrast, during tensile loading, the polymer matrix primarily bears the load, and the beads do not significantly disrupt the material's deformation behavior. Since tensile failure is dominated by crack propagation and elongation rather than crushing, the presence of glass beads has minimal impact on tensile strength. Instead, a slight increase in elongation at break is observed, as the polymer chains accommodate the stress more effectively.

Fig. 12 shows the behavior of SLES material under compressive load at different hardener ratios. SLES was actually used to foam the polyurethane material. A foam form of polyurethane was aimed to be obtained, and this was successful; however, the achieved strength values (0.5 MPa) are insufficient for the bushing materials used in automotive industry. It is considered that it will be used in bushings that operate under lower loads. The amount of material used in the foaming method was reduced by %50. When a %75 strain was applied, the sample fragmented. The material used at the given ratios should not exceed %40 strain. Due to the low strength values under compressive load, tensile tests were not conducted.

3.4. Bushing behavior under dynamic test

According to the results of static compression and tensile tests, P40 material was used for the bushing material. Bushing samples were produced with different amounts of carbon fiber powder added to P40. The samples tested for fatigue were P40, P40KE5, P40KE10, and P40KE15. The fatigue tests were conducted at 4 Hz with a load limit of ±1.8 kN, and load-

displacement data were recorded. In Fig. 13, P40 material was subjected to 1 million cycles under tension and compression. This cycle count is the standard established for bushings used in the automotive sector. No damage occurred in the P40 material after 1 million cycles, and it met the requirements. To reduce visual complexity in the tension-compression cycle curve, the first 20 and last 20 cycles of the total cycles were taken. When examining the load-displacement curve under cycling, it was observed that the strain increased over time at the same load during the tensile phase. As mentioned in the previous static tests, polyurethane material is more sensitive to speed under tensile loading. At high cycling speeds, the stiffness of the material decreased in the tensile region while remaining constant in the compression region. This situation in the tensile region was reduced by adding carbon fiber powder, and it was even eliminated in the sample with %5 carbon fiber powder added. The addition of carbon fiber powder improved the material's time-dependent stable behavior in both the tensile and compression regions. The fatigue load-displacement curves are shown in Fig. 14-16. The addition of carbon powder enhances the dynamic behavior of the sample by stabilizing its stiffness over time through several micro-mechanisms. Firstly, carbon particles improve load transfer within the polymer matrix, distributing stress more evenly and reducing localized stress concentrations, which helps delay material degradation under cyclic loading. Additionally, carbon powder increases internal friction, enhancing energy dissipation and damping, thereby preventing excessive softening. It also acts as a barrier to microcrack growth, bridging, and inhibiting the propagation of cracks that typically develop during repeated loading. Strong interfacial adhesion between the carbon particles and the polymer matrix prevents polymer chain slippage, maintaining structural integrity, and stiffness over extended cycles. Furthermore, carbon powder improves thermal conductivity, dissipating heat generated during cyclic loading and preventing temperature-related polymer softening. These combined effects mitigate fatigue-induced softening, ensuring a more stable dynamic response over prolonged use. The bushings used in this study are particularly suitable for polyurethane material as they operate mainly in the compression region.
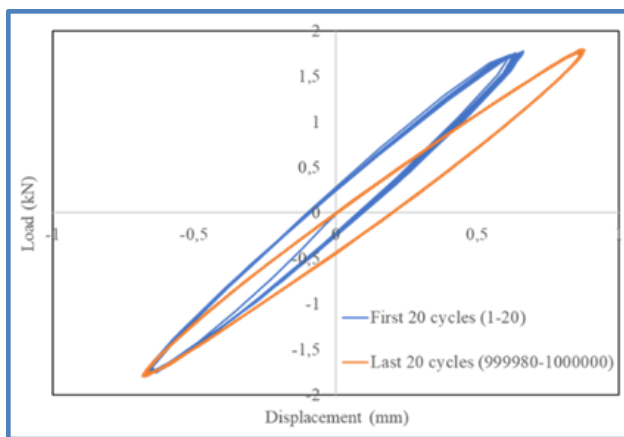

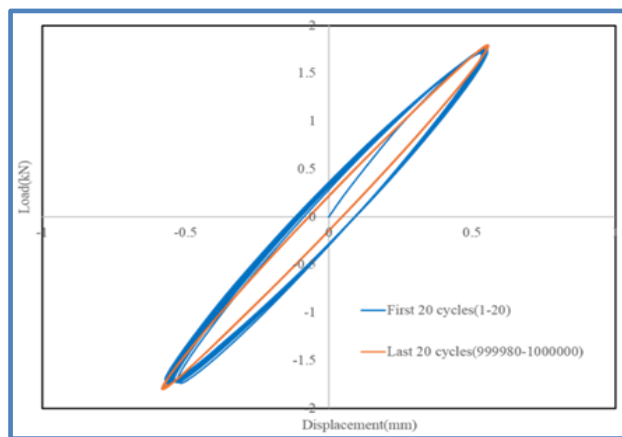**Fig. 13** Tension and compression loading of P40 material at 4 Hz.

Fig. 14 Tension and compression loading of P40KE5 material at 4 Hz.
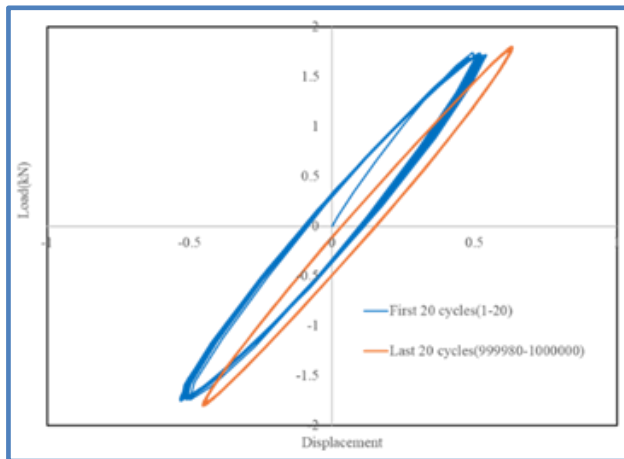
Fig. 15 Tension and compression loading of P40KE10 material at 4 Hz.
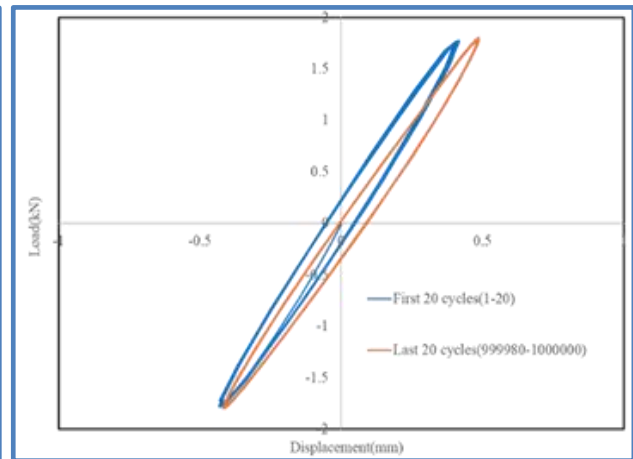

Fig. 16 Tension and compression loading of P40KE15 material at 4 Hz.

4. Conclusion

In this study, the potential use of thermoset polyurethane resins as an alternative to traditional rubbers for bushings used in the automotive sector was investigated. In this context, the behavior of polyurethane material was evaluated for different mixture ratios and additives. Test results showed that the addition of carbon fiber powder increased the strength and ductility of the material. By reinforcing plain polyurethane resin, the performance of the bushing can be enhanced. However, glass beads were found to reduce tensile and compressive strength while increasing the ductility of polyurethane. Since SLES material foamed the polyurethane, the desired strength values used in the project could not be obtained. The tensile strength of polyurethane material increases with an increase in strain rate, but the unit elongation value decreases simultaneously. Generally, polyurethane material is more sensitive to strain rate under tensile loading. When examining fatigue behavior, it was observed that stiffness decreased over time in the tensile region, while it remained constant in the compression region. Production was carried out using the casting method, and the produced bushings passed durability testing. Polyurethane resin can be used as an alternative to traditional rubbers used in the automotive sector.

Declaration

Author Contribution: Conceive-B.E.B., K.C.; Design-K.C., S.G., B.E.B.; Supervision- K.C., S.G., B.E.B.; Computational Performance, Data Collection and/or Processing- P.G., E.B., K.C., A.K., E.K., S.G., B.E.B.; Analysis and/or Interpretation- P.G., E.B., K.C., A.K., E.K., S.G., B.E.B.; Literature Review- P.G., E.B., K.C.; Writer- P.G., E.B., K.C.; Critical Reviews– P.G., E.B., K.C., A.K., E.K., S.G., B.E.B.

Conflict of interests: The authors have declared no conflicts of interest.

Orcid-ID

Pelin Güler https://orcid.org/0009-0007-0779-0120
Egemen Bayramlar https://orcid.org/0009-0007-5625-4084
Kenan Çınar https://orcid.org/0000-0001-7402-2032
Ahmet Kaymaz https://orcid.org/0009-0002-6500-2923
Elçin Kahraman https://orcid.org/0009-0001-0251-3008
Bülent Ecevit Bayram https://orcid.org/0009-0003-5840-2627
Sezer Gelen https://orcid.org/0009-0005-2810-6469

References

[1] W. V. Mars and A. Fatemi, "A literature survey on fatigue analysis approaches for rubbers," *Int. J. Fatigue*, vol. 24, pp. 949–961, 2002.

[2] W. V. Mars and A. Fatemi, "Factors that affect the fatigue life of rubber: A literature survey," *Rubber Chem. Technol.*, vol. 77, pp. 391–412, 2004.

[3] E. Ostoja-Kuczynski and P. Charrier, E. Verron, G. Marckmann, L. Gornet, et al. "Crack initiation in filled natural rubber: experimental database and macroscopic observations," * 3rd European Conference on Constitutive Models for Rubbers*, 2003.

[4] N. Saintier, G. Cailletaud, and R. Piques, "Crack initiation and propagation under multiaxial fatigue in a natural rubber," *Int. J. Fatigue*, vol. 28, no. 1, pp. 61–72, 2006.

[5] P. Ghosh, R. Mukhopadhyay, and R. Stocek, "Durability prediction of NR/BR and NR/SBR blend tread compounds using tear fatigue analyser," *KGK-Kautschuk Gummi Kunststoffe*, vol. 69, no. 6, pp. 53–55, 2016.

[6] Y. Zhou, S. Jerrams, and L. Chen, "Multi-axial fatigue in magnetorheological elastomers using bubble inflation," *Mater. Des.*, vol. 50, pp. 68–71, 2013.

[7] R. J. Harbour, A. Fatemi, and W. V. Mars, "Fatigue crack orientation in NR and SBR under variable amplitude and multiaxial loading conditions," *J. Mater. Sci.*, vol. 43, no. 6, pp. 1783–1794, 2008.

[8] K. Legorju-Jago and C. Bathias, "Fatigue initiation and propagation in natural and synthetic rubbers," *Int. J. Fatigue*, vol. 24, no. 2–4, pp. 85–92, 2002.

[9] J.-B. Le Cam, B. Huneau, and E. Verron, "Description of fatigue damage in carbon black filled natural rubber," *Fatigue Fract. Eng. Mater. Struct.*, vol. 31, no. 12, pp. 1031–1038, 2008.

[10] P. Rublon, B. Huneau, E. Verron, N. Saintier, S. Beurrot, A. Leygue, C. Mocuta, D. Thiaudière, and D. Berghezan, "Multiaxial deformation and strain-induced crystallization around a fatigue crack in natural rubber," *Eng. Fract. Mech.*, vol. 123, pp. 59–69, 2014.

[11] A. Stevenson, "A fracture mechanics study of the fatigue of rubber in compression" *Int. J. Fracture*, vol. 23, pp. 47, 1983.

[12] N. Saintier, G. Cailletaud, and R. Piques, "Cyclic loadings and crystallization of natural rubber: An explanation of fatigue crack propagation reinforcement under a positive loading ratio," *Mater. Sci. Eng. A*, vol. 528, no. 3, pp. 1078–1086, 2011.

[13] A. Zine, N. Benseddiq, and M. N. Abdelaziz, "Rubber fatigue life under multiaxial loading: Numerical and experimental investigations," *Int. J. Fatigue*, vol. 33, no. 10, pp. 1360–1368, 2011.

[14] G. Ayoub, F. Zaïri, M. Naït-Abdelaziz, and J.-M. Gloaguen, "Modeling the low-cycle fatigue behavior of visco-hyperelastic elastomeric materials using a new network alteration theory: Application to styrene-butadiene rubber," *J. Mech. Phys. Solids*, vol. 59, no. 2, pp. 473–495, 2011.

[15] Y.-P. Wu, W. Zhao, and L.-Q. Zhang, "Improvement of flex-fatigue life of carbon-black-filled styrene-butadiene rubber by addition of nanodispersed clay," *Macromol. Mater. Eng.*, vol. 291, no. 8, pp. 944–949, 2006.

[16] G. Berton, C. Cruanes, F. Lacroix, S. Méo, and N. Ranganathan, "Study of the fatigue behavior of the polychloroprene rubber with stress variation tests," *Proc. Eng.*, vol. 101, pp. 413–420, 2015.

[17] J.-L. Poisson, F. Lacroix, S. Meo, G. Berton, and N. Ranganathan, "Biaxial fatigue behavior of a polychloroprene rubber," *Int. J. Fatigue*, vol. 33, no. 8, pp. 1151–1157, 2011.

[18] S. Seichter, V.-M. Archodoulaki, T. Koch, A. Holzner, and A. Wondracek, "Investigation of different influences on the fatigue behaviour of industrial rubbers," *Polym. Test.*, vol. 59, pp. 99–106, 2017.

[19] H. Ismail, K. Muniandy, and N. Othman, "Fatigue life, morphological studies, and thermal aging of rattan powder-filled natural rubber composites as a function of filler loading and a silane coupling agent," *BioResources*, vol. 7, no. 1, pp. 841–858, 2012.

[20] A. Lion and M. Johlitz, "On the representation of chemical ageing of rubber in continuum mechanics," *Int. J. Solids Struct.*, vol. 49, no. 10, pp. 1227–1240, 2012.

[21] M. Johlitz and A. Lion, "Chemo-thermomechanical ageing of elastomers based on multiphase continuum mechanics," *Continuum Mech. Thermodyn.*, 2013, pp. 1–20.

[22] A. Herzig, M. Johlitz, and A. Lion, "An experimental set-up to analyse the oxygen consumption of elastomers during ageing by using a differential oxygen analyser," *Continuum Mech. Thermodyn.*, vol. 27, no. 6, pp. 1009–1018, 2015.

[23] F. E. Ngolemasango, M. Bennett, and J. Clarke, "Degradation and life prediction of a natural rubber engine mount compound," *J. Appl. Polym. Sci.*, vol. 110, no. 1, pp. 348–355, 2008.

[24] V. Vinod, S. Varghese, and B. Kuriakose, "Degradation behaviour of natural rubber-aluminium powder composites: effect of heat, ozone and high energy radiation," *Polym. Degrad. Stab.*, vol. 75, no. 3, pp. 405–412, 2002.

[25] K. Junik et al., "Impact of the hardness on the selected mechanical properties of rigid polyurethane elastomers commonly used in suspension systems," *Eng. Fail. Anal.*, vol. 121, p. 105201, 2021.

[26] K. Junik et al., "Constitutive law identification and fatigue characterization of rigid PUR elastomers 80 ShA and 90 ShA," *Materials*, vol. 15, no. 19, p. 6745, 2022.

[27] M. Cerit, E. Nart, and K. Genel, "Investigation into effect of rubber bushing on stress distribution and fatigue behaviour of anti-roll bar," *Eng. Fail. Anal.*, vol. 17, no. 5, pp. 1019–1027, 2010.